World Academy of Science, Engineering and Technology
International Journal of Aerospace and Mechanical Engineering
Vol:7, No:9, 2013

Adaptive Shape Parameter (ASP) Technique for Local Radial Basis Functions (RBFs) and Their Application for Solution of Navier Strokes Equations

A. Javed, K. Djidjeli, J. T. Xing

Abstract—The concept of adaptive shape parameters (ASP) has been presented for solution of incompressible Navier Strokes equations using mesh-free local Radial Basis Functions (RBF). The aim is to avoid ill-conditioning of coefficient matrices of RBF weights and inaccuracies in RBF interpolation resulting from non-optimized shape of basis functions for the cases where data points (or nodes) are not distributed uniformly throughout the domain. Unlike conventional approaches which assume globally similar values of RBF shape parameters, the presented ASP technique suggests that shape parameter be calculated exclusively for each data point (or node) based on the distribution of data points within its own influence domain. This will ensure interpolation accuracy while still maintaining well-conditioned system of equations for RBF weights. Performance and accuracy of ASP technique has been tested by evaluating derivatives and laplacian of a known function using RBF in Finite difference mode (RBF-FD), with and without the use of adaptivity in shape parameters. Application of adaptive shape parameters (ASP) for solution of incompressible Navier Strokes equations has been presented by solving lid driven cavity flow problem on mesh-free domain using RBF-FD. The results have been compared for fixed and adaptive shape parameters. Improved accuracy has been achieved with the use of ASP in RBF-FD especially at regions where larger gradients of field variables exist.

Keywords—CFD, Meshless Particle Method, Radial Basis Functions, Shape Parameters

I. Introduction

RADIAL Basis Functions were initially developed for multivariate data and function interpolation. However, their true meshfree behaviour has attracted the researchers to employ these for solution of differential equations. In early 90s, Kansa [1] proposed the use of RBFs for solution of Partial Differential Equations (PDEs). Later, various researchers found it useful to apply radial basis function for numerical solution of differential equations on meshfree domains [2]–[7]. RBF approach provides good spectral accuracy. However, coefficient matrices of RBFs tend to become ill-conditioned as the number of data points within the interpolation region increases. This puts severe limitations on number and distribution of data points (or nodes) within the domain. In order to overcome this difficulty, use of local radial basis functions was suggested as an alternative to global basis function [8]–[11]. Local RBF techniques generate sparse and better conditioned coefficient matrices by compromising on spectral accuracy of the solution. RBF in Finite Difference mode (RBF-FD) [9]–[12] and RBF based differential quadrature methods (RBF-DQ) [8] are the two famous local RBF techniques which are used for solution of Navier Stroke's equations in meshfree domain.

Accuracy of RBF interpolation mainly depends upon the *flatness* of basis function. Huage et al [13] suggested that accuracy of interpolation can be improved by making the basis function flatter. On the other hand, an increased flatness of basis function results in higher condition number of coefficient matrix. Large condition number of coefficient matrix of RBF weights causes inaccuracies in the solution for expansion coefficients coefficient [1]. Therefore, choice of basis function should be a balance between flatness and conditioning of coefficient matrices.

It has been known that behaviour of basis functions (especially for Multi-quadratic and inverse multi-quadratic) depends heavily of choice of shape parameter. Wang [5] stated that the sensitivity of results with choice of shape parameter was one of the biggest limitation of RBF. Various researchers have presented different methodologies to find the optimum values of shape parameters for RBFs [5], [13]–[15]. Franke [7] suggested optimal value of shape parameter based on total number of neighbouring particles and minimum diameter enclosing all the neighbouring particles around the data point. Rippa [15] studied the selection of optimal shape parameter for RBFs and concluded that a scheme for determining good value of shape parameter should take the number and distribution of data points, radial basis function, condition number of coefficient matrix and precision of computation into account. For any particular interpolation problem, the radial basis function and precision of computation remains similar throughout the domain. However, if the distribution of data points is not uniform, the optimal value of shape parameter will differ for each data point in local RBFs and would depend upon the number and distribution of data points within its own influence domain.

Lately, RBF interpolation has been used for solution of fluid flow problems using meshfree methods [6], [8], [11], [16]. For such applications the nodal distribution is required to be

A. Javed is with CED Group, Faculty of Engineering and Environment, University of Southampton, SO171BJ, Southampton, United Kingdom(Phone +44-7534354285, email: A.Javed@soton.ac.uk)

K. Djidjeli is with CED Group, Faculty of Engineering and Environment, University of Southampton, SO171BJ, Southampton, United Kingdom (email: kkd@soton.ac.uk)

J. T. Xing is with FSI Group, Faculty of Engineering and Environment, University of Southampton, SO171BJ, Southampton, United Kingdom (email: jtxing@soton.ac.uk)

TABLE I
COMMONLY USED RADIAL BASIS FUNCTIONS

Type of radial basis function	Expression of $\phi(r)$
Multi-quadratic (MQ)	$\phi(r) = \sqrt{r^2 + \sigma^2}$
Inverse Multi-quadratic (IMQ)	$\phi(r) = 1/\sqrt{r^2 + \sigma^2}$
Inverse Quadratic (IQ)	$\phi(r) = 1/(r^2 + \sigma^2)$
Gaussian (GA)	$\phi(r) = \exp(-(\sigma r)^2)$

varied within the domain to have higher nodal density at the regions where larger gradients of field variables are expected. In these cases, use of globally similar value of shape function may not ensure well-conditioned coefficient matrix throughout the domain. Therefore, accuracy of the solution would vary within the domain accordingly. For highly non-uniform nodal distribution, the resultant ill conditionings in the coefficient matrices dominate the solution causing significant inaccuracies in the values of expansion coefficients(λ). These inaccuracies result in breakdown of solution during subsequent iteration process [14]. Therefore, severe limitations are imposed on the use of non-uniform or random particle distribution within the domain.

In order to address this problem, the concept of adaptive shape parameter (ASP) is presented. The presented approach suggests calculation of exclusive value of shape parameter (σ) at each data point (or node). The value would depend upon number and distribution of neighbouring particles in the influence domain. Incompressible Navier Strokes equations, in vorticity-stream function formulation, are solved using the approach. The authors have observed that in addition to improved accuracy of interpolation, use of adaptive shape parameter (ASP) also allows larger variation of nodal density within the domain. Therefore, much refined grids can be placed at regions experiencing larger gradients of field variables without introducing ill-conditioning effects.

II. RBF FORMULATION

For N scattered data points$(x_i)\epsilon\mathbf{R}^{d+1}, 1 \leq i \leq N$, the approximation $\bar{\mathbf{u}}(x)$ to a real valued function $\mathbf{u}(x)$ using Radial Basis Function (RBF) is written as:

$$\bar{\mathbf{u}}(x) = \sum_{i=1}^{N} \lambda_i \phi(\|x - x_i\|), \qquad x\epsilon\mathbf{R}^d \tag{1}$$

where $\phi(\|x - x_i\|)$ is a radial basis function, $\|.\|$ is a standard Euclidean norm and λ_i is the expansion coefficient. Some of the common radial basis functions have been defined in Table I. The unknown parameter $\lambda_i = 1, 2, \ldots N$ can be obtained by setting $\bar{\mathbf{u}}(x_i) = \mathbf{u_i}, i = 1, 2, \ldots N$. This leads to the system of linear equations:

$$A\underline{\lambda} = U \tag{2}$$

where, $\underline{\lambda} = \{\lambda_1, \lambda_2, ...\lambda_N\}^T, U = \{u_1, u_2, ...u_N\}^T$ and $A_{i,j} = \phi(\|x_j - x_i\|)$

A. RBF in Finite Difference Mode (RBF-FD)

As mentioned before, local RBFs have been proposed to overcome the shortcomings of global RBFs. One of the local RBF techniques suggests using RBF in Finite Difference Mode

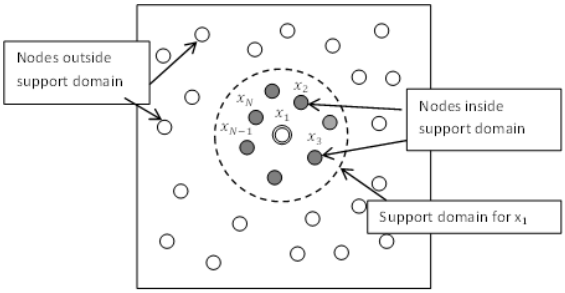

Fig. 1. Support domain of a reference node

(the so called RBF-FD method). The scheme was introduced by Tolstykh et al [9] and Wright et al [12] and has been found highly effective in solving fluid flow problems [11]. The same scheme has been used for the study of Adaptive Shape Parameter (ASP). RBF-FD method directly approximates the derivative of field variables to be used in differential equations.

The idea of RBF-FD method has been derived from Finite Difference method which suggests that derivative of any field variable at a spatial location i can be approximated using the values of field variable at surrounding data points. For this purpose, the interior and boundary of domain is represented by a set of scattered data points. A supporting stencil is identified for each data point by choosing N neighbouring particles. RBF-FD weights are then calculated for any differential operator $\mathcal{L}$, at each data point, by setting up local RBF interpolation.

Using classical finite difference approach, the derivative of any parameter $\mathbf{u}$ at any node, say x_1, can be expressed as

$$\mathcal{L}\mathbf{u}(x_1) = \sum_{j=1}^{N} \mathbf{W}_{1,j}^{(\mathcal{L})} u(x_j) \tag{3}$$

where N is the number of nodes in the support domain of node x_1, $\mathbf{u}(x_j)$ is the value of parameter $\mathbf{u}$ at node x_j and $\mathbf{W}_{1,j}^{(\mathcal{L})}$ is the weight of corresponding differential operator $\mathcal{L}$ at node x_j for node x_1 as shown in figure 1.

Recall that the standard RBF interpolation for a set of distinct points $x_j\epsilon\mathbf{R}^d, j = 1, 2, ...N$ is given by [12]:

$$\mathbf{u}(x) \approx s(x) = \sum_{j=1}^{N} \lambda_j \phi(\|x - x_j\|) + \beta \tag{4}$$

where λ_j and β are the expansion coefficient. Equation (4) can be written in Lagrange form as:

$$\bar{s}(x) = \sum_{j=1}^{N} \mathcal{X}(\|x - x_j\|)\, u(x_j) \tag{5}$$

where $\mathcal{X}(\|x - x_j\|)$ satisfies the cardinal conditions as

$$\mathcal{X}(\|x_k - x_j\|) = \begin{cases} 1, & \text{if } k = j \\ 0, & \text{if } k \neq j \end{cases} \qquad k = 1, 2, ...N \tag{6}$$

Applying the differential operator $\mathcal{L}$ on equation (5) at node x_1 we have:

$$\mathcal{L}u(x_1) \approx \mathcal{L}\bar{s}(x_1) = \sum_{j=1}^{N} \mathcal{L}\mathcal{X}(\|x_1 - x_j\|)\, u(x_j) \tag{7}$$

Using equations (3) and (7), RBF-FD weights $\mathbf{W}_{1,j}^{(\mathcal{L})}$ are given by

$$\mathbf{W}_{1,j}^{(\mathcal{L})} = \mathcal{L}\mathcal{X}\left(\|x_1 - x_j\|\right) \tag{8}$$

The weights can be computed by solving the following linear system [11]:

$$\begin{bmatrix} \Phi & e \\ e^T & 0 \end{bmatrix} \begin{bmatrix} W \\ \mu \end{bmatrix} = \begin{bmatrix} \mathcal{L}\phi_1 \\ 0 \end{bmatrix} \tag{9}$$

where $\Phi_{i,j} = \phi\left(\|x_j - x_i\|\right), i,j = 1,2,\ldots,N$, $e_i = 1,2,\ldots,N$, $\mathcal{L}\phi_1$ represents the column vector $\mathcal{L}\phi_1 = [\mathcal{L}\phi\|x - x_1\|\mathcal{L}\phi\|x - x_2\|\ldots\mathcal{L}\phi\|x - x_N\|]^T$ evaluated at node x_1 and μ is a scalar parameter which enforces the condition:

$$\sum_{j=1}^{N} \mathbf{W}_{1,j}^{(\mathcal{L})} = 0 \tag{10}$$

Equation (9) can be written in matrix form as:

$$[A]\{\mathrm{W}\} = \{\mathcal{L}\phi\} \tag{11}$$

Evaluation of equation (11) at each node x_1 gives weights $\mathbf{W}_{1,j}^{\mathcal{L}}$ of all the nodes in the support domain for particular differential operator $\mathcal{L}$. Corresponding weights and location of nodes in support domains are then used to approximate the complete differential equation at node x_1. However, solution of equation (11) requires that coefficient matrix $[A]$ be non-singular. Moreover, matrix needs to be well-conditioned so as to avoid inaccuracies resulting from computation process. The possibility of having a non-singular and well-conditioned coefficient matrix $[A]$ depends upon the type of radial basis function and corresponding value of shape parameter used for the problem [15].

Using ASP technique, the value of shape parameter (σ) would separately be calculated for each row of coefficient matrix. Therefore, $\Phi_{i,j} = \phi\left(\|x_j - x_i\|, \sigma_i\right), i = 1,2,\ldots,N$. This would reduces the condition number of the matrix for the problems where nodal distribution is not uniform within the domain. As mentioned earlier, various models have suggested for finding good value of shape parameters [5], [7], [13]–[15], [17]. For present study, a commonly used scheme, presented by Franke [7] has been used which suggests optimum shape parameter as $\sigma_i = (1.25D_i)/\sqrt{N_i}$ where, σ_i is the shape parameter value of node i, N_i is the number of neighbouring particles (within the influence domain) and D_i is the minimum diameter of circular enclosing all the neighbouring particles. Other schemes for calculating optimum shape parameters can also be tested to further validate the concept of ASP.

B. RBF-FD for Incompressible N-S Equations

Vorticity Stream function formulation of two dimensional Navier Strokes equations in non-dimensionalized form can be expressed as:

$$\frac{\partial\omega}{\partial t} + u\frac{\partial\omega}{\partial x} + v\frac{\partial\omega}{\partial y} = \frac{1}{Re}\left(\frac{\partial^2\omega}{\partial x^2} + \frac{\partial^2\omega}{\partial y^2}\right) \tag{12}$$

$$\frac{\partial^2\psi}{\partial x^2} + \frac{\partial^2\psi}{\partial y^2} = -\omega \tag{13}$$

Cartesian velocity components can be obtained from derivatives of stream function as:

$$u = \frac{\partial\psi}{\partial y} \tag{14}$$

$$v = -\frac{\partial\psi}{\partial x} \tag{15}$$

Spatial derivatives appearing in equations (12) and (13) can be approximated using RBF-FD as:

$$\frac{\partial\omega_i}{\partial t} + u_i\sum_{j=1}^{N}\mathbf{W}_{i,j}^{(x)}\omega_j + v_i\sum_{j=1}^{N}\mathbf{W}_{i,j}^{(y)}\omega_j = \frac{1}{Re}\left(\sum_{j=1}^{N}\mathbf{W}_{i,j}^{(xx)}\omega_j + \sum_{j=1}^{N}\mathbf{W}_{i,j}^{(yy)}\omega_j\right) \tag{16}$$

$$\sum_{j=1}^{N}\mathbf{W}_{i,j}^{(xx)}\psi_j + \sum_{j=1}^{N}\mathbf{W}_{i,j}^{(yy)}\psi_j = -\omega_i \tag{17}$$

Temporal discretization of equation (16) can be obtained using Crank Nicolson scheme as under:

$$\begin{aligned}\frac{\omega_i^{n+1} - \omega_i^n}{\delta t} = {} & \frac{1}{2Re}\left(\sum_{j=1}^{N}\mathbf{W}_{i,j}^{(xx)}\omega_j^{n+1} + \sum_{j=1}^{N}\mathbf{W}_{i,j}^{(yy)}\omega_j^{n+1}\right) \\ & -\frac{1}{2}\left(u_i\sum_{j=1}^{N}\mathbf{W}_{i,j}^{(x)}\omega_j^{n+1} + v_i\sum_{j=1}^{N}\mathbf{W}_{i,j}^{(y)}\omega_j^{n+1}\right) \\ & \frac{1}{2Re}\left(\sum_{j=1}^{N}\mathbf{W}_{i,j}^{(xx)}\omega_j^{n} + \sum_{j=1}^{N}\mathbf{W}_{i,j}^{(yy)}\omega_j^{n}\right) \\ & -\frac{1}{2}\left(\sum_{j=1}^{N}\mathbf{W}_{i,j}^{(x)}\omega_j^{n} + v_i\sum_{j=1}^{N}\mathbf{W}_{i,j}^{(y)}\omega_j^{n}\right)\end{aligned} \tag{18}$$

where ω_j^n and ω_j^{n+1} are the values of ω at node j at n^{th} and $(n+1)^{th}$ time step respectively. After rearrangement, equation (18) can be expressed in matrix form as:

$$\begin{bmatrix} a_{1,1}+1 & a_{1,2} & \ldots & a_{1,N} \\ a_{2,1} & \ddots & \ldots & \vdots \\ \vdots & \ldots & \ddots & \vdots \\ a_{N,1} & a_{N,2} & \ldots & a_{N,N}+1 \end{bmatrix} \begin{Bmatrix} \omega_1^{n+1} \\ \omega_2^{n+1} \\ \vdots \\ \omega_N^{n+1} \end{Bmatrix} = \begin{bmatrix} b_{1,1}+1 & b_{1,2} & \ldots & b_{1,N} \\ b_{2,1} & \ddots & \ldots & \vdots \\ \vdots & \ldots & \ddots & \vdots \\ b_{N,1} & b_{N,2} & \ldots & b_{N,N}+1 \end{bmatrix} \begin{Bmatrix} \omega_1^{n} \\ \omega_2^{n} \\ \vdots \\ \omega_N^{n} \end{Bmatrix} \tag{19}$$

where

$$a_{i,j} = -\frac{\delta t}{2}\left\{\frac{1}{Re}\left(\sum_{j=1}^{N}\mathbf{W}_{i,j}^{(xx)} + \sum_{j=1}^{N}\mathbf{W}_{i,j}^{(yy)}\right) - u_i\sum_{j=1}^{N}\mathbf{W}_{i,j}^{(x)} - v_i\sum_{j=1}^{N}\mathbf{W}_{i,j}^{(y)}\right\}$$

$$b_{i,j} = \frac{\delta t}{2}\left\{\frac{1}{Re}\left(\sum_{j=1}^{N}\mathbf{W}_{i,j}^{(xx)} + \sum_{j=1}^{N}\mathbf{W}_{i,j}^{(yy)}\right) - u_i\sum_{j=1}^{N}\mathbf{W}_{i,j}^{(x)} - v_i\sum_{j=1}^{N}\mathbf{W}_{i,j}^{(y)}\right\}$$

Similarly, equation (17) can be written in matrix form as:

$$\begin{bmatrix} \mathbf{W}_{1,1}^{(xx)} + \mathbf{W}_{1,1}^{(yy)} & \dots & \mathbf{W}_{1,N}^{(xx)} + \mathbf{W}_{1,N}^{(yy)} \\ \mathbf{W}_{2,1}^{(xx)} + \mathbf{W}_{2,1}^{(yy)} & \ddots & \vdots \\ \vdots & \dots & \vdots \\ \mathbf{W}_{N,1}^{(xx)} + \mathbf{W}_{N,1}^{(yy)} & \dots & \mathbf{W}_{N,N}^{(xx)} + \mathbf{W}_{N,N}^{(yy)} \end{bmatrix} \begin{Bmatrix} \psi_1 \\ \psi_2 \\ \vdots \\ \psi_N \end{Bmatrix} = -\begin{Bmatrix} \omega_1 \\ \omega_2 \\ \vdots \\ \omega_N \end{Bmatrix} \quad (20)$$

Velocity components at each node can be evaluated as:

$$u_i = \sum_{j=1}^{N}\mathbf{W}_{i,j}^{(y)} \quad (21)$$

$$v_i = -\sum_{j=1}^{N}\mathbf{W}_{i,j}^{(x)} \quad (22)$$

An iterative process for solving equations (19-22) can be followed starting with initial conditions of vorticity and stream function. During each time step, equation (20) can be solved to find the values of stream function (ψ) at each node. The values of stream function can then be used to find velocity components using equations (21) and (22). Finally, value of vorticity at next time step can be calculated by solving by solving the linear system (19).

III. Numerical Tests

A. Calculation of Derivatives and Laplacians of a Known Function

Performance of adaptively shaped radial basis functions in finite difference mode, has been tested by calculating 1st and 2nd derivatives and laplacian of a known function over meshfree domain. For this purpose, evaluation of function $f(x,y) = sin\,[3(x-2.5)(y-2.5)]$ has been considered over a 2D domain with dimensions $[0.5 \quad 4.5] \times [0.5 \quad 4.5]$.

The function, its first derivative and laplacian have been plotted in Figure 2(a) to 2(c) respectively. It can be observed that the gradients and laplacian values of function are rather uniform in the middle of the domain. However, towards the edges and corners, sharp gradients are encountered. Therefore, an efficient meshing strategy should consider having higher nodal density towards corners which gradually coarsens while moving towards the middle of the domain. Hence, a 60x60 non-uniform particle distribution (as shown in Figure 3) has been chosen for calculation of gradients using RBF-FD method.

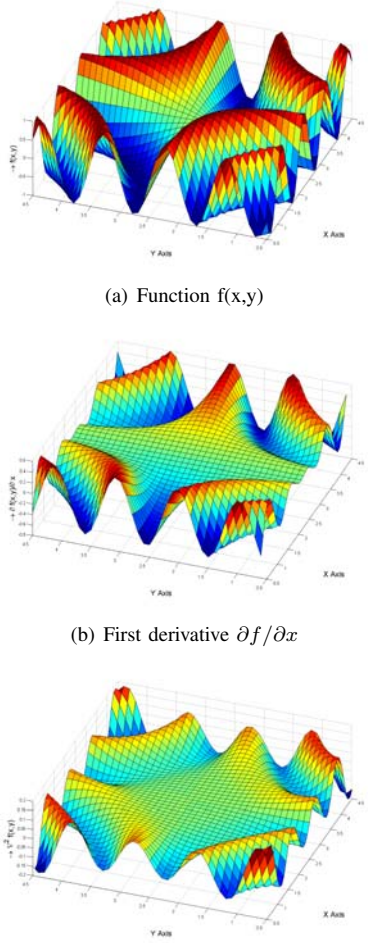

(a) Function f(x,y)

(b) First derivative $\partial f/\partial x$

(c) Laplacian $\nabla^2 f$

Fig. 2. Plot of Pre assumed function, derivative and Laplacian

Figure 4 shows the optimum values of σ over the entire domain using the criterion identified by Franke [7]. The figure indicates that optimum values change by almost 400 percent across various regions of the domain. Therefore, use of globally similar values will likely cause inaccuracies. The derivatives of given function have been calculated using globally similar values of σ as well as using ASP technique. The absolute error has been calculated for each approach by comparing the results with known values of derivatives of function $f(x,y)$. Figures 5 and 6 show the error values of $\partial f/\partial x$ and $\nabla^2 f$ respectively, along the diagonal line (shown as thick line in figure 3) through the domain. Calculations have been done using Multiquadratic and Inverse Multiquadratic radial basis functions. For constant values of σ the results have been obtained using three different values ($\sigma = 0.5$,$\sigma = 1.0$

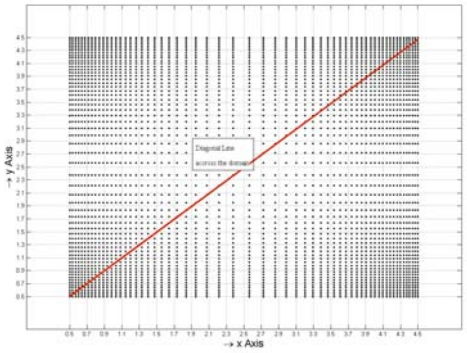

Fig. 3. 60x60 Non-uniforms Nodal Distribution within the Domain

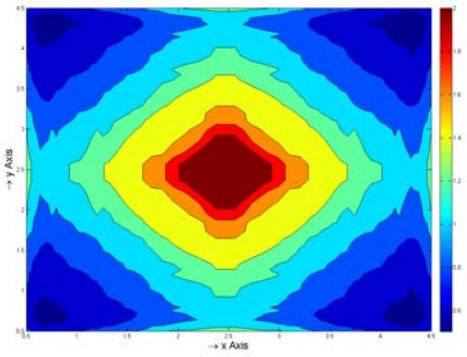

Fig. 4. Profile of Optimum Values of Shape Parameter (σ)

and $\sigma = 2.0$) and compared with ASP results to have better understanding of how results behave with varying the value of shape parameter.

Figure 3 shows that density of nodes varies along the diagonal line from maximum (at bottom left corner) to minimum (in the middle) and then again to maximum (at top right corner). Therefore, optimum value of σ should vary accordingly. The plots in figures 5 and 6 show that, for fixed value of shape parameter (σ), the results are accurate only on partial range of the diagonal. Therefore, global accuracy is not achieved. However, adaptively varying the shape parameters (using ASP technique) results in good agreement with the analytical values throughout the range. For example, $\sigma = 0.5$ provides good accuracy close to corners but the results tend to become erroneous in the middle of the domain. As the value of σ is increased from 0.5 to 2.0, the large error region tends to shift towards the corners. This is due to the deviation from the suggested optimum value of shape parameter at various regions (Figure 4) that causes these errors.

In order to further explain the situation, curve of $\nabla^2 f$ has been plotted in Figure 7. It can be observed, in closed views, that RBF curve with fixed shape parameter tends to deviate from analytical values near the central part of the domain. However, the curve obtained by adaptively changing the shape parameter tends to closely follow the analytical value curve. Therefore, globally accurate results are achieved with adaptively changing the shape of the basis function according to the arrangement of neighbouring particles around the data points.

B. Lid Driven Cavity Flow

Lid driven cavity flow constitutes complex flow features like primary, secondary and tertiary eddies despite the fact that it has very simple geometry. The flow problem is therefore widely used to validate new computational techniques and novel schemes for flow simulations. Therefore, application of ASP for RBF-FD has been validated by simulating lid driven cavity flow in a square and comparing the results with the bench mark solutions for this problem presented by Ghia et al [18]. Flow conditions at Reynolds number 400 and 1000 are considered for the numerical simulations. The fluid domain has been represented by 6561 and 10201 nodes (or particles) for Re 400 and Re 1000 cases respectively. The domain has been non-dimensionalized to acquire standardized numerical values. The solutions have been obtained for constant as well as adaptively shaped radial basis functions. Non-uniform particle distribution has been introduced to capture higher gradients expected near solid walls and corners.

On all the four walls, velocity components normal to boundary are assumed to be zero. This ensures no penetration of flow across the boundary Γ. This leads to $\vec{u}_n = \partial\psi/\partial\vec{t} = 0$ or $\psi = C_1$ at $x\epsilon\Gamma$, where $\vec{u}_n$ is the velocity component in the outward normal direction to the boundary $(\Gamma), n$ and t are normal and tangential directions to the boundary and C_1 is a constant. No slip boundary condition at the walls implies that tangential component of flow velocity along the boundary Γ remains constant and equal to the speed of the boundary itself. Therefore, $\vec{u}_t = \partial\psi/\partial\vec{n} = C_2$ at $x\epsilon\Gamma$, where $\vec{u}_t$ is the velocity component parallel to the boundary (Γ) and C_2 is a constant. The values of stream function (ψ) near the boundary can be used to define the boundary conditions for vorticity (ω). Higher order finite difference expressions for vorticity at the four boundaries can therefore be expressed as [19]:

$$Left: \omega_{i,j} = -\frac{3}{h}\left[v_{i,j} + \frac{\psi_{i+1,j} - \psi_{i,j}}{h} + \frac{h}{6}\omega_{i+1,j}\right] \quad (23)$$

$$Right: \omega_{i,j} = \frac{3}{h}\left[v_{i,j} + \frac{\psi_{i,j} - \psi_{i-1,j}}{h} - \frac{h}{6}\omega_{i-1,j}\right] \quad (24)$$

$$Top: \omega_{i,j} = -\frac{3}{h}\left[v_{i,j} + \frac{\psi_{i,j} - \psi_{i,j-1}}{h} + \frac{h}{6}\omega_{i,j-1}\right] \quad (25)$$

$$Bottom: \omega_{i,j} = \frac{3}{h}\left[v_{i,j} + \frac{\psi_{i,j} - \psi_{i,j+1}}{h} - \frac{h}{6}\omega_{i,j+1}\right] \quad (26)$$

For lid driven cavity flow, all the boundaries are stationary except the top boundary which moves with a velocity U_0 in horizontal direction. Implementation of boundary conditions using equations (23 - 26) necessitates the presence of locally orthogonal grid near the boundary. For uniform particle distribution, condition of locally orthogonal grid is implicitly met. However, for random particle distribution, inner particles may not remain orthogonal to the boundary. Therefore, special care

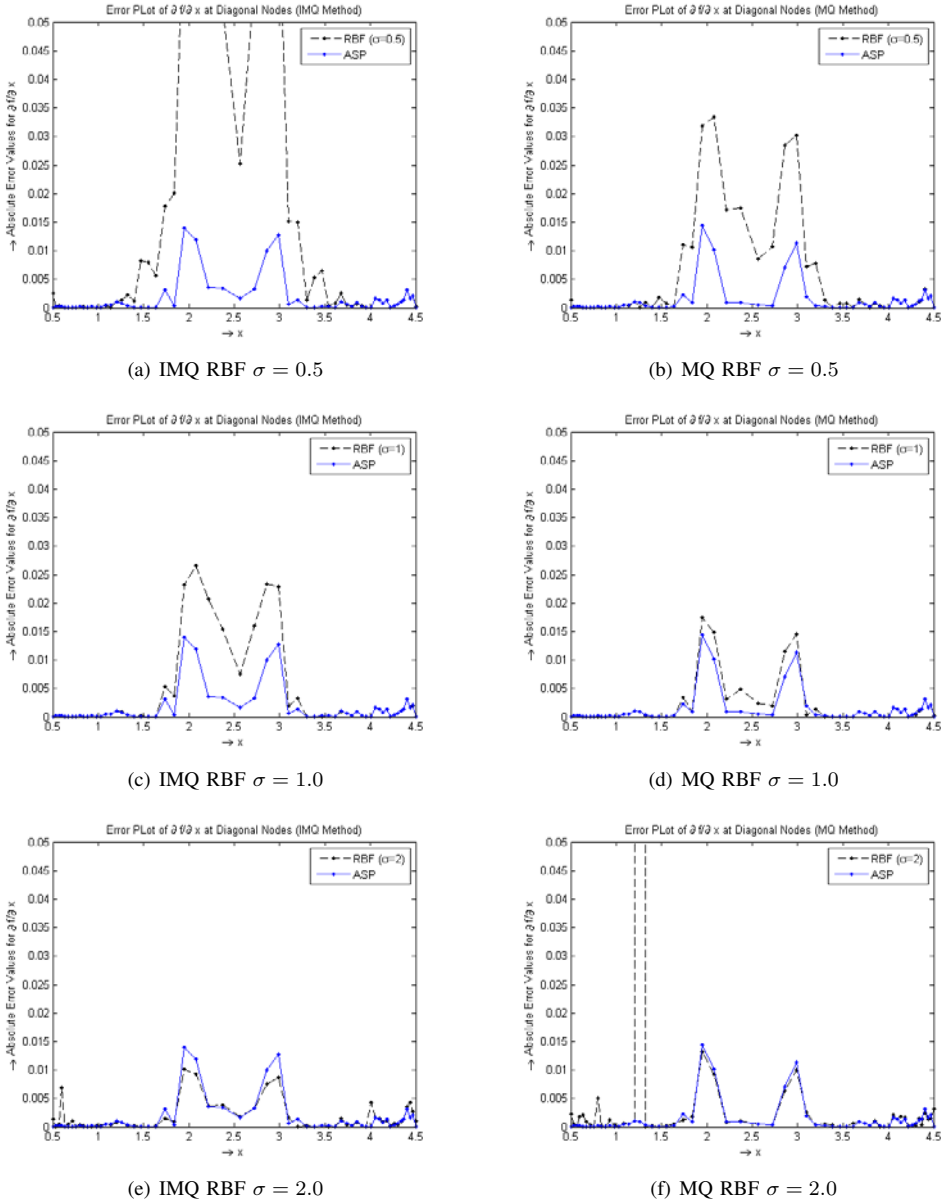

(a) IMQ RBF $\sigma = 0.5$ (b) MQ RBF $\sigma = 0.5$

(c) IMQ RBF $\sigma = 1.0$ (d) MQ RBF $\sigma = 1.0$

(e) IMQ RBF $\sigma = 2.0$ (f) MQ RBF $\sigma = 2.0$

Fig. 5. Error Plots of $\partial f/\partial x$ along Diagonal Line through the Domain for MQ and IMQ RBFs (Fixed and Adaptively Changing Values of shape parameter σ)

has to be taken to ensure locally orthogonal grid near the boundary. At steady state, higher gradients of flow velocities are experienced near the walls. Therefore, non-uniform grid spacing with finer grid near the walls will improve the accuracy. In case of constant value of shape parameter (σ), the ratio of nodal spacing between corner-to-centre nodes is limited due to ill-conditioning effect of coefficient matrix for RBF weights in equation (11) as discussed in section II(A). However, with introduction of adaptively shaped radial basis functions, the ratio of nodal spacing between corner-to-centre nodes can be increased without producing ill-conditioning effect. The grid can therefore be made more refined, close to the walls, than same sized grid used for fixed shape parameter approach. The results are therefore more accurate for same number of nodes within the domain. Figures 8(a) and 8(b) show the nodal distributions for fixed and adaptive shape parameter cases at Re 400. Due to the ill-conditioning effect with the use of fixed shape parameters, the ratio of nodal spacing between corner-to-centre nodes was limited to 4.0 only. Further refinement near the walls and corners resulted in inaccurate RBF-FD weights leading to erroneous solutions with the use of conventional RBF-FD approach. However, ratio of nodal spacing between corner-to-centre nodes could be increased to 8.0 with the use of adaptively shaped basis functions. Therefore much refined nodal distribution was obtained close to the corners as shown in figure 8(b). Finer grids were able to capture the gradients of field variables more accurately. Moreover, with the use of ASP, optimized shape of basis function was maintained

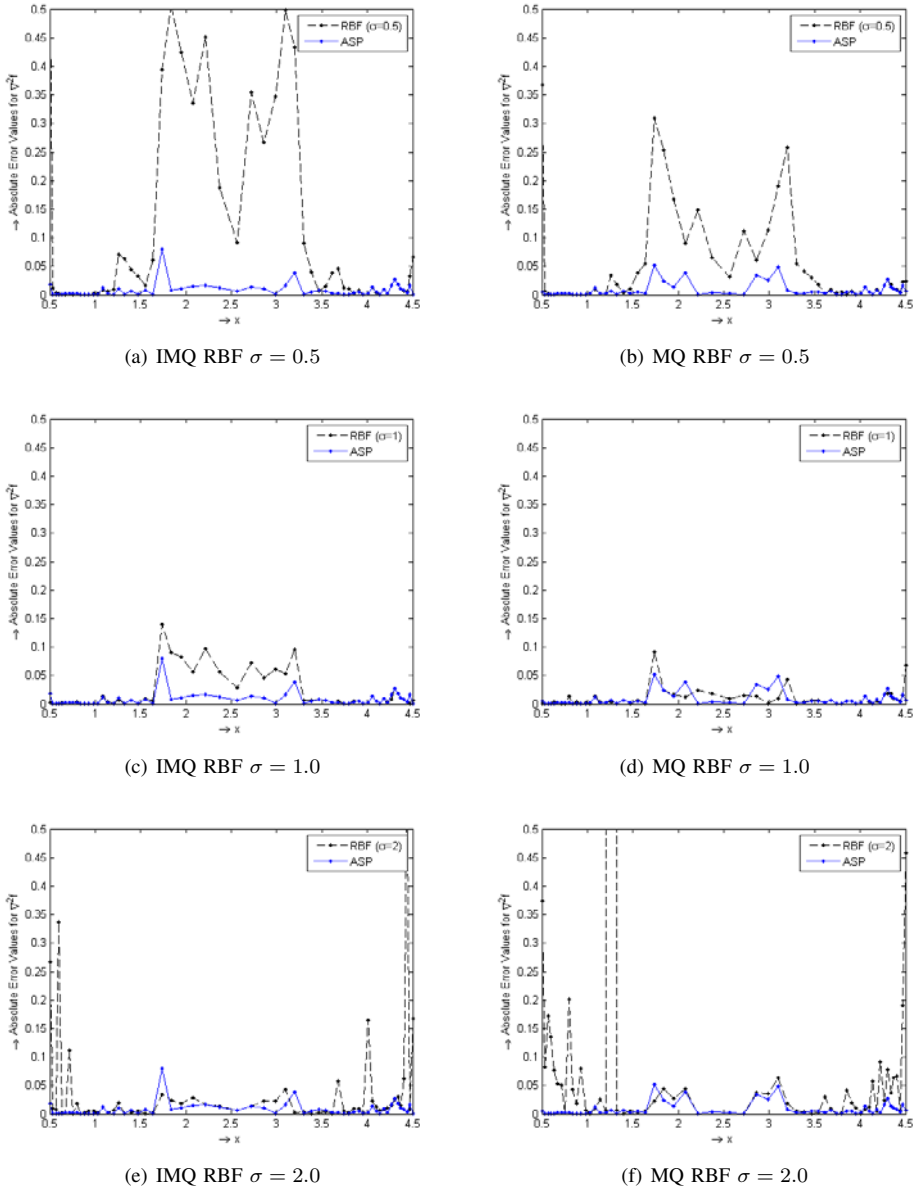

(a) IMQ RBF $\sigma = 0.5$ (b) MQ RBF $\sigma = 0.5$

(c) IMQ RBF $\sigma = 1.0$ (d) MQ RBF $\sigma = 1.0$

(e) IMQ RBF $\sigma = 2.0$ (f) MQ RBF $\sigma = 2.0$

Fig. 6. Error Plots of $\nabla^2 f$ along Diagonal Line through the Domain for MQ and IMQ RBFs (Fixed and Adaptively Changing Values of shape parameter σ)

throughout the domain thus reducing the error. As a result, an improved accuracy was achieved with adaptively shaped RBF-FD. Figures 9(a) and 9(b) show profile of horizontal velocity component (v_x) at mid span and vertical velocity component (v_y) at mid plane respectively, for Re 400 case. The results have been obtained using adaptively shaped RBF-FD. Similar velocity profiles have been calculated for Re 1000 and shown in Figures 10(a) and 10(b), respectively. Figures 11(a) and 11(b) show vorticity (ω) profiles at Re 400 and 1000, respectively.

In table II, a comparison of results obtained from fixed and adpatively shaped RBF-FD has been presented by evaluating the error values using standard results from Ghia et al [18]. Maximum relative error and norm of relative error for fixed and adaptive shape parameter cases have been shown. It can be observed that significant reduction in error is achieved with the use of adaptively shaped basis functions. This is due to the possibility of having finer grids at critical regions and accurate approximation of gradients due to optimized shape of basis functions.

IV. Conclusion

The concept of adaptive shape parameters (ASP) is found useful for flow simulations where solutions are sought through local RBF techniques and nodal density is required to be varied significantly within the domain to capture higher gradients. Adaptively shaped basis functions provide greater flexibility to change the nodal density thus enabling an improved accuracy. Moreover, the basis functions can retain their optimum shape throughout the domain and produce accurate approximations

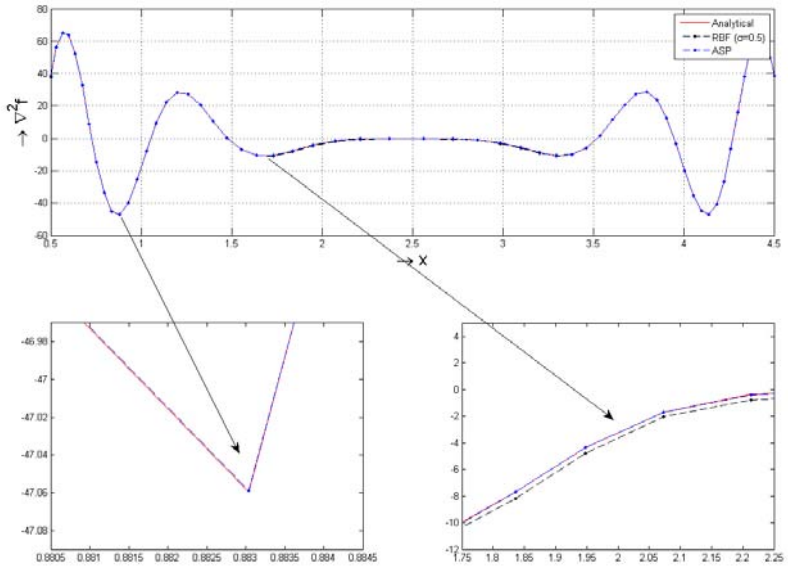

Fig. 7. Comparison of Laplacian ($\nabla^2 f$) Curves along the diagonal

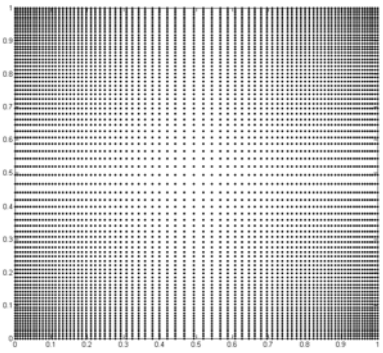

(a) For fixed shape parameter σ

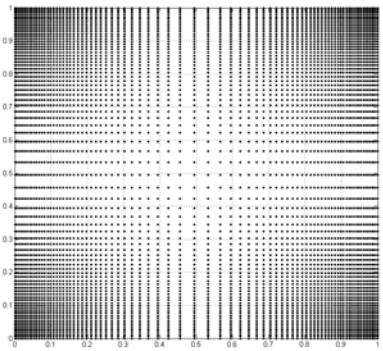

(b) For adaptive shape parameter σ

Fig. 8. Arrangement of nodes for lid driven cavity flow problem

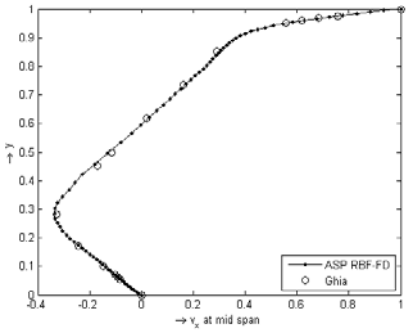

(a) v_x at mid span

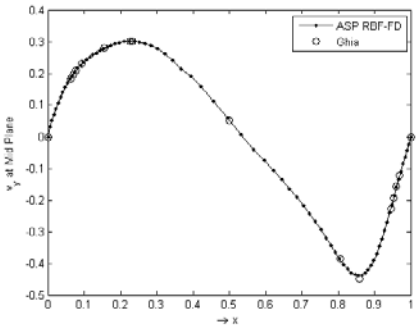

(b) v_y at mid plane

Fig. 9. Velocity profiles for lid driven cavity flow at Re 400 solved with adaptively shaped RBF-FD method

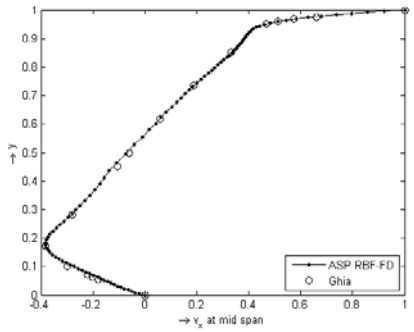

(a) v_x at mid span

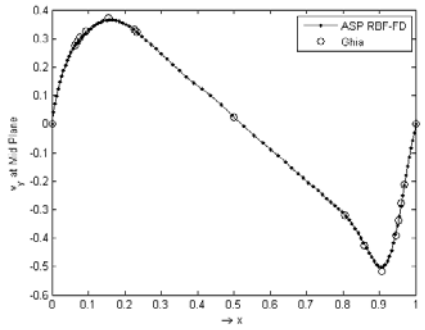

(b) v_y at mid plane

Fig. 10. Velocity profiles for lid driven cavity flow at Re 1000 solved with adaptively shaped RBF-FD method

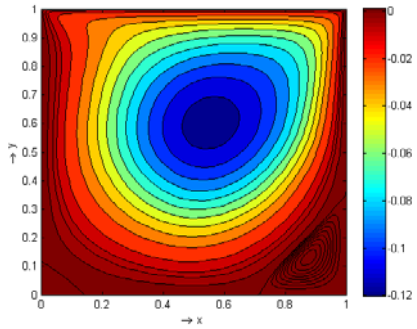

(a) For Re 400

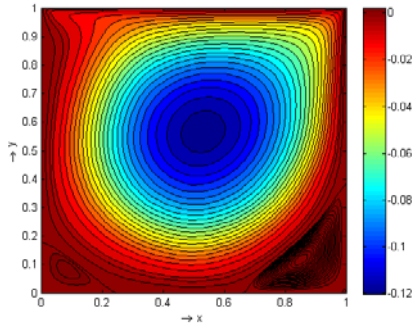

(b) For Re 1000

Fig. 11. Vorticity (ω) plots for lid driven cavity flow solved with adaptively shaped RBF-FD method

TABLE II
MAXIMUM ERROR AND NORM OF ERROR FOR RE 400 AND RE 1000 WITH FIXED AND ADAPTIVELY SHAPED BASIS FUNCTIONS

Case	Fixed RBF-FD	Adaptive RBF-FD
Results for v_x at mid span		
Max relative error (Re 400)	0.0372	0.0150
Norm of relative error (Re 400)	0.0787	0.0203
Max relative error (Re 1000)	0.0459	0.0250
Norm of relative error (Re 1000)	0.2071	0.1104
Results for v_y at mid plane		
Max relative error (Re 400)	0.0404	0.0089
Norm of relative error (Re 400)	0.1121	0.0556
Max relative error (Re 1000)	0.0439	0.0156
Norm of relative error (Re 1000)	0.1190	0.0549

of differential operators. On the contrary, the conventional approach of using fixed shaped basis functions results in ill-conditioning effect when large variation of nodal density is introduced within the domain. Therefore, grid refinement is required to be introduced over the entire domain so as to avoid large variation in nodal spacing at different locations. This practice increases total number of data points (or nodes) thus making the solutions computationally expansive. Therefore, use of ASP with local RBFs helps improve the computational efficiency and accuracy in these cases.

REFERENCES

[1] E. J. Kansa, "Multiquadrics - a scattered data approximation scheme with applications to computational fluid-dynamics .2. solutions to parabolic, hyperbolic and elliptic partial-differential equations," *Computers and Mathematics with Applications*, vol. 19, no. 8-9, pp. 147–161, 1990.

[2] W. Chen and M. Tanaka, "A meshless, integration-free, and boundary-only rbf technique," *Computers and Mathematics with Applications*, vol. 43, no. 3-5, pp. 379–391, 2002.

[3] M. C. V. Bayona, M. Moscoso and M. Kindelan, "Rbf-fd formulas and convergence properties," *Journal of Computational Physics*, vol. 229, no. 22, pp. 8281–8295, 2010.

[4] N. Mai-Duy and T. Tran-Cong, "Numerical solution of differential equations using multiquadric radial basis function networks," *Neural Networks*, vol. 14, no. 2, pp. 185–199, 2001.

[5] J. G. Wang and G. R. Liu, "On the optimal shape parameters of radial basis functions used for 2-d meshless methods," *Computer Methods in Applied Mechanics and Engineering*, vol. 191, no. 23-24, pp. 2611–2630, 2002.

[6] K. D. P. Phani Chinchapatnam and P. B. Nair, "Radial basis function meshless method for the steady incompressible navierstokes equations," *International Journal of Computer Mathematics*, vol. 84, no. 10, pp. 1509–1521, 2007.

[7] C. Franke and R. Schaback, "Solving partial differential equations by collocation using radial basis functions," *Applied Mathematics and Computation*, vol. 93, no. 1, pp. 73–82, 1998.

[8] H. D. C. Shu and K. S. Yeo, "Local radial basis function-based differential quadrature method and its application to solve two-dimensional incompressible navier-stokes equations," *Computer Methods in Applied Mechanics and Engineering*, vol. 192, no. 7-8, pp. 941–954, 2003.

[9] A. I. Tolstykh and D. A. Shirobokov, "On using radial basis functions in a "finite difference mode" with applications to elasticity problems," *Computational Mechanics*, vol. 33, no. 1, pp. 68–79, 2003.

[10] Y. Sanyasiraju and G. Chandhini, "Local radial basis function based gridfree scheme for unsteady incompressible viscous flows," *Journal of Computational Physics*, vol. 227, no. 20, pp. 8922–8948, 2008.

[11] P. B. N. P. Phani Chinchapatnam, K. Djidjeli and M. Tan, "A compact rbf-fd based meshless method for the incompressible navier-stokes equations," *Proceedings of the Institution of Mechanical Engineers Part M-Journal of Engineering for the Maritime Environment*, vol. 223, no. M3, pp. 275–290, 2009.

[12] G. B. Wright and B. Fornberg, "Scattered node compact finite difference-type formulas generated from radial basis functions," *Journal of Computational Physics*, vol. 212, no. 1, pp. 99–123, 2006.

[13] C. F. L. C. S. Huang and A. H. D. Cheng, "Error estimate, optimal shape factor, and high precision computation of multiquadric collocation method," *Engineering Analysis with Boundary Elements*, vol. 31, no. 7, pp. 614–623, 2007.
[14] L. I. M. Gherlone and M. D. Sciuva, "A novel algorithm for shape parameter selection in radial basis functions collocation method," *Composite Structures*, vol. 94, no. 2, pp. 453–461, 2012.
[15] S. Rippa, "An algorithm for selecting a good value for the parameter c in radial basis function interpolation," *Advances in Computational Mathematics*, vol. 11, no. 2-3, pp. 193–210, 1999.
[16] A. G. S. Hamed Meraji and P. Malekzadeh, "An efficient algorithm based on the differential quadrature method for solving navier-stokes equations," *International Journal for Numerical Methods in Fluids*, pp. n/a–n/a, 2012.
[17] R. Franke, "Scattered data interpolation: Tests of some method," *Mathematics of Computation*, vol. 38, no. 157, pp. 181–200, 1982.
[18] U. K. N. G. Ghia and C. Shin, "High-re solutions for incompressible flow using the navier-stokes equations and a multigrid method," *Journal of Computational Physics*, vol. 48, no. 3, pp. 387 – 411, 1982.
[19] W. F. Spotz and G. F. Carey, "High-order compact scheme for the steady stream-function vorticity equations," *International Journal for Numerical Methods in Engineering*, vol. 38, no. 20, pp. 3497–3512, 1995.

Ali Javed is a PhD research student at Computational Engineering and Design Group, Faculty of Engineering and Environment, University of Southampton, UK. He is a graduate in Aerospace Engineering and has done his Masters in Solid Mechanics before starting the PhD. Presently he is doing research in Meshless Particle Methods and their applications to Fluid Structure Interaction problems. In that, he is investigating the use of local Radial Basis Functions (RBF) for modelling and simulation of flows around fluctuating / moving bodies. He is also employing Arbitrary Lagrangian Eulerian (ALE) solution schemes on hybrid meshfree-mesh based grids to develop an efficient solver for analysing flow induced vibrations of cylindrical bodies and aerofoils at various Reynolds Numbers.

Kamal Djidjeli is lecturer in Computational Methods in the Computational Engineering and Design Group, Faculty of Engineering and the Environment at the University of Southampton. He obtained his MSc and PhD degrees in Computational methods from University of West London, Brunel UK in 1988 and 1991. He joined the Faculty of Engineering, University of Southampton in 1991 as Research Fellow and become academic staff Lecturer and Admission Director of Maritime Engineering Science MSc Programme and Exams Officer in the Faculty of Engineering, University of Southampton. Since 1995, he has taught courses on advanced numerical methods, computational fluid dynamics, applications of CFD, Design Search and Optimization, Powered lift, high performance computing, mathematics and computing to students in the School of Engineering Sciences at the undergraduate and MSc levels. He has over 20 years research experience in the area of numerical analysis and computational engineering. He has published over 50 papers in refereed journals and conferences, and has supervised a number of MSc and PhD students (about 25). His current research is on particle meshless methods for fluid flow and fluid structure interaction problems, and energy harvesting. His other contributions include numerical methods for fluid-structure modelling, computational fluid dynamics, nonlinear dynamical systems and chaos, and water waves. He is a referee for a number of journals (Computers and Fluids, International Journal for Numerical Methods in Engineering, Journal of Computational Physics, Journal of Aircraft-AIAA, Applied Mathematics and Computation, Journal of Computational and Applied Mathematics, etc) and has undertaken a range of research projects such as UKIERI (UK-India Education and Research Initiative), Lloyds Register London collaborative project, industrial projects (Larsen and Toubro Ltd, India), etc addressing fluid structure interactions, fluid flow and free surface flows using CFD, wing in ground effect vehicles, etc. Dr. Djidjeli serves on the editorial board member of the ISRN Applied Mathematics Journal. He is member of the American Institute of Aeronautics and Astronautics (AIAA), and the Institute of Mathematics and its applications, UK.

Jing Tang Xing is an Emeritus Professor in the Fluid Structure Interaction Group, the Faculty of Engineering and the Environment at the University of Southampton. He obtained his doctoral degree in fluid-solid interaction dynamics from Tsinghua University, Beijing China in 1984. He joined the Faculty of Engineering, Mathematics and Science, University of Southampton in 1993. Professor Xing has a broad range of research interests and contributions in theoretical and applied continuum dynamics, computational modelling, fluid-solid interactions and vibration and controls. A major thrust of Professor Xings current research is in fluid-structure interaction dynamics. He has made significant contributions to the development of the mixed finite element substructuresubdomain method for linear fluid-structure problems, and the mixed finite element finite difference method for nonlinear fluid-solid interaction modelling. His publication record includes over 200 journal/conference papers and technical research reports. As the principal / a joint investigator of EPSRC and European Projects, he has successfully managed many research grants. He is a fellow of the Institute of Mathematics and its applications, C. Math.